

Oxygen-Barrier Properties of Copolymers Based on Ethylene Terephthalate

A. POLYAKOVA,¹ R. Y. F. LIU,¹ D. A. SCHIRALDI,² A. HILTNER,¹ E. BAER¹

¹Department of Macromolecular Science and Center for Applied Polymer Research, Case Western Reserve University, 10900 Euclid Avenue, Cleveland, Ohio 44106

²KOSA, 1551 Sha Lane, Spartanburg, South Carolina 29304

Received 8 November 2000; revised 15 May 2001; accepted 18 May 2001

ABSTRACT: The oxygen-barrier properties of amorphous polyethylene terephthalate-based copolymers with various acid comonomers were examined. The incorporation of increasing amounts of isophthalate, phthalate, or naphthalate gradually reduced the permeability P toward the low values obtained for the corresponding homopolymers. The permeability of poly(ethylene 3,4'-bibenzoate) homopolymer was only slightly lower than that of polyethylene terephthalate, and the copolymers correspondingly exhibited a very gradual decrease in P as the amount of 3,4'-bibenzoate (3,4'BB) increased. In contrast, copolymerization with the linear isomer, 4,4'BB, produced a substantial increase in P . Generally, comonomer affected the solubility S less than the diffusivity D , and therefore changes in P reflected primarily changes in D for the polymers studied. The diffusivity and solubility depended on the copolymer composition in accordance with static and dynamic free-volume concepts of gas permeability in glassy polymers. The solubility S correlated with the amount of free volume as determined by the glass-transition temperature. Correlation of the diffusivity D with the magnitude of the subambient γ relaxation identified dynamic free volume with thermally activated conformational changes and segmental motions. Correspondence in the activation energy confirmed the relationship. © 2001 John Wiley & Sons, Inc. *J Polym Sci Part B: Polym Phys* 39: 1889–1899, 2001

Keywords: polyethylene terephthalate; copolyesters; glassy state; free volume; oxygen diffusion; gas barrier; dynamic mechanical relaxation

INTRODUCTION

Polyethylene terephthalate (PET) is widely used in a range of high-barrier applications because of its low cost and good mechanical properties. However, there is a continuing practical need to improve the PET barrier. Crystallization and orientation are two approaches to barrier enhancement. The efficient packing of chains in lamellar crystals¹ or in the ordered regions of oriented

PET² reduces the available free volume to the extent that these regions are considered impermeable.

Copolymerization offers an alternative and possibly complementary approach to the barrier enhancement of PET. The gas permeability of aromatic polymers and copolymers consistently decreases when the *para*-phenylene linkage is replaced by a *meta*- or *ortho*- linkage.³ This trend has been demonstrated^{4–10} for various polysulfones, polyimides, polyesters, and poly(phenolphthalein phthalates). Chain symmetry appears to affect both the thermodynamic (solubility) and kinetic (diffusivity) components of permeability.

Correspondence to: A. Hiltner (E-mail: pah6@po.cwru.edu)

Journal of Polymer Science: Part B: Polymer Physics, Vol. 39, 1889–1899 (2001)
© 2001 John Wiley & Sons, Inc.

However, the relationship between polymer structure and gas barrier is only partially understood.

There is general agreement that lower gas solubility of asymmetric isomers reflects lower free volume relative to the symmetric counterpart. This is consistent with the lower glass-transition temperature (T_g) and higher density and is attributed to better packing of asymmetric polymers in the glassy and melt states.^{4,6} Conceptually, the relationship of chain symmetry to diffusivity appears to be less clear. The effect of asymmetry on chain flexibility has often been considered.¹¹ Indeed, a relationship between gas transport and subambient relaxation processes in glassy polymers was suggested some time ago.¹² Such a correlation was subsequently demonstrated for diffusivity of some polyesters,⁹ but more recent attempts to correlate permeability with subambient relaxation behavior gave ambiguous results;³ consequently, this promising avenue of investigation has been largely abandoned in favor of free-volume concepts of diffusivity.^{13,14}


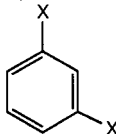
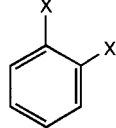
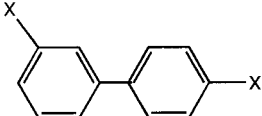
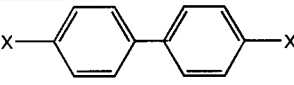
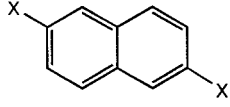
In the present study, the oxygen barrier of PET-based copolymers was investigated to establish relationships with chain structure. Copolymerization with terephthalate isomers (isophthalate and phthalate) inserted kinks and bends in the chain without changing the molecular weight and chemical composition of the repeat unit. The effect of asymmetry was explored further by comparing copolymers with 3,4'-bibenzoate (3,4'BB) and 4,4'-BB. Copolymers with 2,6-naphthalate were also included in this study to probe the effect of comonomer size on barrier properties. In most cases, copolymers were examined over the entire composition range. Oxygen solubility and diffusivity were correlated with other physical properties and interpreted in terms of established polymer physics concepts. Subsequent contributions will compare oxygen-barrier properties of a larger variety of comonomer structures and examine the effect of an impermeable crystalline or oriented phase on the oxygen barrier of PET copolymers.

EXPERIMENTAL

Synthesis of PET Homopolymer

All the polymers were supplied by KOSA (Spartanburg, SC). The detailed procedure for the synthesis of PET homopolymer has been described.¹

Table I. Structure and Designation of Acid Repeat Units for PET-Based Copolymers

Structure	Designation
$X = \text{---} \begin{array}{c} \text{O} \\ \parallel \\ \text{C} \\ \diagup \quad \diagdown \\ \text{O} \quad \text{O} \end{array}$ 	Terephthalate (T)
	Isophthalate (I)
	Phthalate (P)
	3,4'-Bibenzoate (3,4'BB)
	4,4'-Bibenzoate (4,4'BB)
	Naphthalate (N)

To prepare the copolymers, the process was repeated, maintaining a total amount of dicarboxylic acid esters of 4.0 mols. Thus, for example, to produce a copolymer of PET with 10 mol % isophthalate, 3.6 mols of dimethyl terephthalate and 0.4 mols of dimethyl isophthalate were utilized. Randomization of comonomers was virtually ensured under the melt-polymerization process that is utilized in the current study.¹⁵ All the polymers were polymerized to the same level of melt viscosity at 10 rpm agitation rate. Intrinsic viscosities of 0.64 ± 0.03 dL g⁻¹ were measured for the laboratory-scale copolymers based on the coefficient for PET homopolymer. Because the polyesters were living condensation polymers, polydispersities of approximately 2.0 were always obtained under conditions of melt equilibration. The structure and designation of the repeat units of the copolymers are summarized in Table I.

Table II. Barrier Properties of Polyesters

Material	Copolymer Content (%)	T_g DMTA, 0.1 Hz (°C)	Amorphous Density (g cm ⁻³)	Temperature (°C)	P^a	D^b	S^c	Specific Free Volume (cm ³ g ⁻¹)
PET	100	81	1.3350	10	0.253 ± 0.003	2.3 ± 0.1	0.117 ± 0.003	0.033
				25	0.469 ± 0.002	5.6 ± 0.2	0.098 ± 0.002	0.027
				40	0.743 ± 0.004	11.6 ± 0.2	0.068 ± 0.001	0.019
PET-I	2.5	81	1.3359	25	0.451 ± 0.004	5.2 ± 0.1	0.099 ± 0.002	0.028
				25	0.430 ± 0.006	5.0 ± 0.1	0.099 ± 0.002	0.028
				25	0.398 ± 0.010	4.7 ± 0.2	0.098 ± 0.004	0.027
				25	0.357 ± 0.008	4.4 ± 0.1	0.094 ± 0.004	0.026
				25	0.298 ± 0.003	3.8 ± 0.2	0.091 ± 0.001	0.025
PEI	100	68	1.3509	10	0.211 ± 0.005	2.9 ± 0.2	0.084 ± 0.004	0.023
				25	0.059 ± 0.004	0.6 ± 0.1	0.109 ± 0.004	0.030
				25	0.099 ± 0.010	1.6 ± 0.1	0.072 ± 0.003	0.020
PET-P	2.5	81	1.3363	25	0.152 ± 0.005	3.6 ± 0.2	0.049 ± 0.002	0.014
				25	0.440 ± 0.003	5.2 ± 0.1	0.096 ± 0.002	0.027
				25	0.402 ± 0.010	4.9 ± 0.1	0.095 ± 0.002	0.026
				25	0.387 ± 0.002	4.8 ± 0.3	0.093 ± 0.004	0.026
				25	0.364 ± 0.010	4.7 ± 0.2	0.089 ± 0.004	0.025
				25	0.341 ± 0.005	4.6 ± 0.1	0.086 ± 0.003	0.024
				25	0.281 ± 0.006	4.2 ± 0.1	0.077 ± 0.004	0.021
PET-N	50.0	62	1.3410	25	0.250 ± 0.002	2.5 ± 0.2	0.116 ± 0.004	0.032
				25	0.180 ± 0.008	3.2 ± 0.2	0.065 ± 0.003	0.018
				25	0.415 ± 0.003	4.8 ± 0.2	0.099 ± 0.003	0.028
				25	0.409 ± 0.003	4.5 ± 0.1	0.105 ± 0.002	0.029
				25	0.404 ± 0.001	4.4 ± 0.2	0.105 ± 0.003	0.029
				25	0.390 ± 0.006	4.3 ± 0.2	0.105 ± 0.004	0.029
PET-N	25.0	96	1.3338	25	0.343 ± 0.002	3.7 ± 0.1	0.106 ± 0.004	0.029
				25	0.250 ± 0.002	2.5 ± 0.2	0.116 ± 0.004	0.032
				25	0.187 ± 0.003	1.6 ± 0.2	0.127 ± 0.005	0.035
				25	0.187 ± 0.003	1.6 ± 0.2	0.127 ± 0.005	0.035
				25	0.187 ± 0.003	1.6 ± 0.2	0.127 ± 0.005	0.035
PEN	100	128	1.3321	10	0.059 ± 0.002	0.6 ± 0.1	0.138 ± 0.003	0.038
				25	0.157 ± 0.001	1.4 ± 0.1	0.134 ± 0.006	0.037
				40	0.352 ± 0.003	3.3 ± 0.2	0.115 ± 0.005	0.032
				25	0.449 ± 0.008	5.3 ± 0.1	0.099 ± 0.002	0.028
				25	0.425 ± 0.007	4.8 ± 0.2	0.102 ± 0.003	0.028
PET-3,4'BB	10	85	1.3326	25	0.410 ± 0.007	4.5 ± 0.3	0.104 ± 0.002	0.029
				25	0.389 ± 0.005	4.3 ± 0.1	0.105 ± 0.004	0.029
				25	0.389 ± 0.005	4.3 ± 0.1	0.105 ± 0.004	0.029
PE3,4' BB	100	100	1.3307	25	0.390 ± 0.004	4.3 ± 0.2	0.113 ± 0.003	0.031
PET-4,4'BB	10	88	1.3307	25	0.390 ± 0.004	4.3 ± 0.2	0.113 ± 0.003	0.031
				25	0.512 ± 0.004	5.5 ± 0.2	0.107 ± 0.002	0.030
				25	0.574 ± 0.005	6.1 ± 0.2	0.109 ± 0.004	0.030
PET-4,4'BB	25	94	1.3228	25	0.574 ± 0.005	6.1 ± 0.2	0.109 ± 0.004	0.030
				25	0.683 ± 0.008	6.9 ± 0.1	0.115 ± 0.003	0.032

^a P—permeability [cc(STP) cm m⁻² atm⁻¹ day⁻¹].

^b D—diffusivity [$\times 10^{13}$ m² s⁻¹].

^c S—solubility [cc(STP) cm⁻³ atm⁻¹].

Polymer Characterization

The amorphous density ρ_a of PET and PET copolymers was determined on 50- μ m-thick compression-molded films. The polymers were dried *in vacuo* at 120 °C for 24 h. To obtain amorphous films, dried pellets were placed between 20- \times 20-cm platens covered with Kapton film. The platens were heated in a press at 265 °C for 1.5 min; pressure was applied, released, reapplied, and held for 1.5 min. The platens were removed from the press and quenched in cold water.

A density gradient column was constructed from a solution of calcium nitrate/water in accordance with ASTM-D 1505 Method B. The column was calibrated with glass floats of known densities. A small piece (\sim 50 mm²) of film was placed in the column and allowed to equilibrate for 10 min before the measurement was taken. The average of three measurements is reported in Table II. The accuracy was \pm 0.0005 g cm⁻³.

Barrier specimens were compression-molded. The pellets were dried *in vacuo* at 120 °C for 24 h

prior to processing. Dried pellets were placed in the 15- × 15-cm cavity of a 150- μm -thick metal spacer and sandwiched between 20- × 20-cm steel platens covered with Teflon-coated aluminum foil. The platens were placed in a press and heated at 265 °C for 5 min with no pressure. Pressure was applied and released; this cycle was repeated three times to ensure that the plaques would be free of air bubbles. Finally, the platens were held under pressure for 5 min and quenched in cold water.

Oxygen flux, $J(t)$, at 0% relative humidity, 1 atm pressure, and 25 °C unless indicated otherwise, was measured with a MOCON OX-TRAN® 2/20. A mixture of 98% N_2 with 2% H_2 was used as the carrier gas, and 100% oxygen was used as the test gas. Prior to testing, specimens were conditioned in nitrogen inside the unit for a minimum of 24 h to remove traces of atmospheric oxygen. Conditioning was especially important for measuring the nonsteady-state oxygen flux from which the diffusivity D was determined. The conditioning was continued until a steady baseline was obtained where the oxygen flux changed by less than 1% for a 30-min cycle. Subsequently, oxygen was introduced to the test cell. The test ended when the flux reached a steady state where the oxygen flux changed by less than 1% during a 30-min test cycle.

The average thickness, l , of each specimen was determined after the barrier measurement was completed. A 7.5- × 7.5-cm square was cut from the tested area, weighed, and the area was determined with a ruler. The average thickness was calculated as $l = W(A\rho)^{-1}$ where W is the sample weight, A is the sample area, and ρ is the density.

Dynamic mechanical measurements were carried out in a DMTA Mk II unit from Polymer Laboratories (Amherst, MA) operating in the tensile mode. Specimens approximately 200 μm thick were compression-molded following the procedure used to prepare barrier specimens. Measurements were taken at frequencies of 1.0 and 0.1 Hz; the temperature was raised from -150 °C through the T_g at a heating rate of 3 °C min^{-1} .

RESULTS AND DISCUSSION

Oxygen-Barrier Properties

Typical experimental $J(t)$ curves in Figure 1 describe the oxygen flux through films of amorphous polyethylene terephthalate (PET), polyethylene

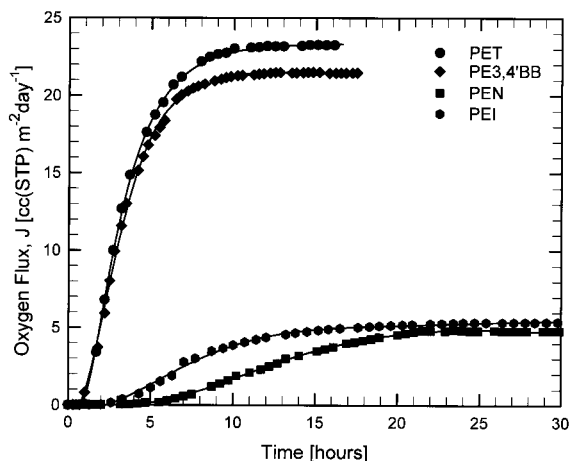


Figure 1. Experimental oxygen-flux data and the fit to Fick's law for amorphous PET, PE3,4'BB, PEI, and PEN.

isophthalate (PEI), polyethylene naphthalate (PEN), and poly(ethylene 3,4'-biphenylene) (PE3,4'BB) homopolymers. Careful conditioning and appropriate choice of specimen thickness resulted in excellent resolution of the various features of the time dependence. The initial increase in oxygen flux reflected nonsteady-state diffusion. This part of the curve was determined mainly by diffusivity D . As the permeant concentration in the specimen reached a constant distribution, the flux reached the steady-state value J_o . This value normalized by film thickness l and permeant gas pressure p defined the permeability $P = J_o l p^{-1}$.

Substitution of terephthalate with isophthalate or naphthalate in the polymer structure had a strong effect on both the nonsteady-state and steady-state parts of the oxygen-flux curve. The nonsteady-state region broadened (slower diffusion) as the steady-state permeability decreased dramatically. Substitution of terephthalate with 3,4'BB had little effect on either the nonsteady-state or the steady-state oxygen flux. Compared with PET, the nonsteady-state region broadened slightly, whereas the steady-state flux decreased slightly.

To obtain diffusivity D and to accurately determine permeability P , the data were fit to the solution of Fick's second law with the appropriate boundary conditions:

$$J(t) = \frac{Pp}{l} \left[1 + 2 \sum_{n=1}^{\infty} (-1)^n \exp\left(-\frac{D\pi^2 n^2 t}{l^2}\right) \right] \quad (1)$$

The fitting curves are included with the experimental points in Figure 1. The fit was excellent

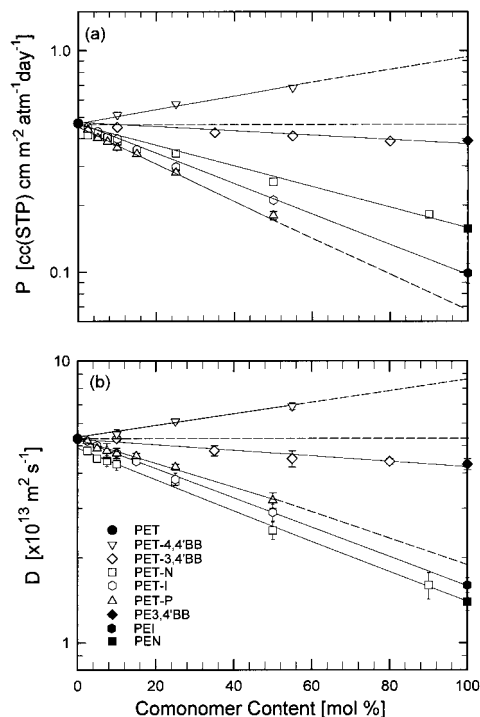


Figure 2. Effect of copolymer composition on (a) logarithm of oxygen permeability and (b) logarithm of oxygen diffusivity.

for all the experiments in the study. As indicated previously, the error in determining the two fitting parameters, Pl^{-1} and DI^{-2} , was estimated not to exceed 2%.¹ Thus, the main source of error in calculating P and D from the experimental flux curves lies in the determination of film thickness l . The low sensitivity of the diffusional flux to thickness variation was demonstrated previously.¹ Therefore, the accuracy of P and D was determined mainly by the accuracy of the average thickness measurement. For this reason, special attention was paid to the average thickness measurement as described in the experimental section. Solubility S was obtained from the relationship $S = PD^{-1}$.

The incorporation of increasing amounts of isophthalate, phthalate, or naphthalate into PET gradually reduced P toward the low values obtained for PEI and PEN homopolymers [see Fig. 2(a)]. The PE3,4'BB homopolymer had a permeability only slightly lower than that of PET, and the copolymers correspondingly exhibited a very gradual decrease in P as the amount of 3,4'BB increased. In contrast, copolymerization with the symmetrical linear isomer, 4,4'BB, produced a substantial increase in P . This was contrary to a

previous report of a substantial decrease in the permeability of PET-4,4'BB copolymers,¹⁶ possibly reflecting a significant orientation effect with the rigid-rod comonomer. Qualitatively, changes in diffusivity paralleled changes in permeability [see Fig. 2(b)]. The change in D was approximately logarithmic with copolymer composition.

The composition dependence of the solubility in Figure 3(a) shows that isophthalate and phthalate decreased S , whereas naphthalate, 3,4'BB and 4,4'BB increased S . The changes were approximately linear with composition. Generally, comonomer affected S less than D , and therefore changes in P reflected primarily changes in D for the copolymer systems studied. Thus, P of isophthalate and phthalate copolymers decreased primarily because of the decrease in D , but also to some extent because S decreased. The large decrease in P of PET-N and smaller decrease in P of PET-3,4'BB copolymers reflected decreases in D . The effect was only slightly offset by the simultaneous increase in S . The increase in P of PET-4,4'BB copolymers was due to increases in both D and S .

Solubility Coefficient and Free Volume

The change in solubility S with copolymer composition paralleled the change in T_g (Fig. 3). Both S

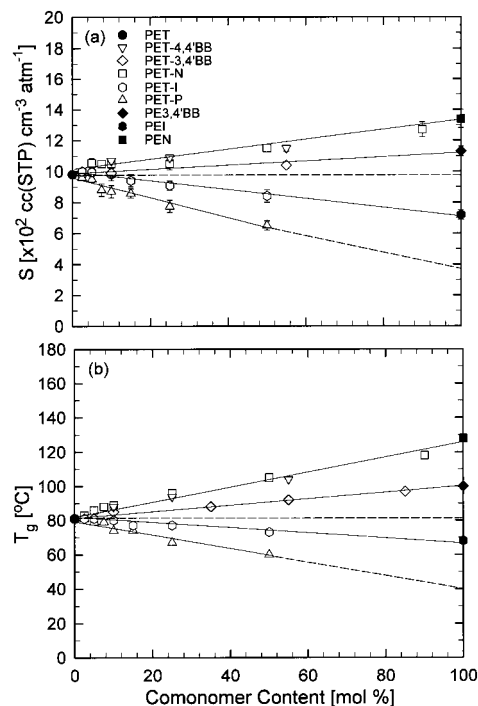


Figure 3. Effect of copolymer composition on (a) oxygen solubility and (b) T_g .

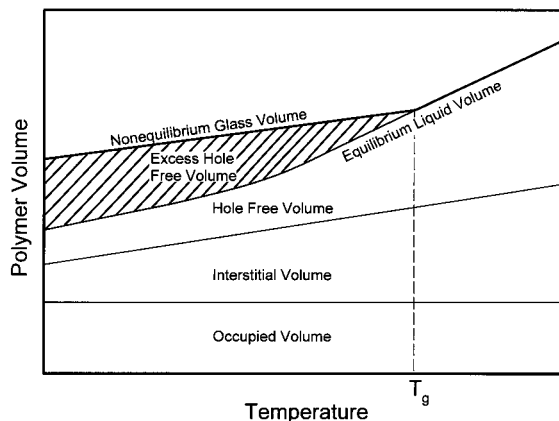


Figure 4. Representation of the volume–temperature relationship for an amorphous polymer following the concepts of Vrentas and Duda.²¹

and T_g varied linearly with composition. The asymmetrical isomers of terephthalate (isophthalate and phthalate) decreased T_g and S . Naphthalate and bibenzoate increased T_g and S , although the symmetrical 4,4' isomer produced a larger change than the asymmetrical 3,4' isomer. There are other examples of aromatic polyesters and poly(ester sulfone)s where the asymmetrical isomers have a significantly lower T_g than the symmetrical isomers,^{9,11,17} and this may be a general phenomenon.³ Possibly, better packing of kinked chains in the melt permits a higher melt density to be achieved before the chains become immobile.

The correlation between S and T_g is consistent with free-volume concepts of gas solubility in glassy polymers. Free volume is a unifying molecular-scale concept that is generally accepted for the structural interpretation of transport properties.¹⁸ In simplified terms, the permeation of small gas molecules through a glassy polymer is viewed as proceeding by jump motion whereby a permeant molecule spends most of the time in free-volume cavities and occasionally jumps into a neighboring cavity. The jump motion proceeds by formation of a channel between two neighboring holes.¹⁹ Thus, gas permeation depends on the number and size of cavities in the polymer matrix (static free volume) and the frequency of channel formation (dynamic free volume). Static free volume is essentially independent of the thermally accessible motions of the macromolecules and relates to gas solubility. Dynamic free volume derives from accessible conformational changes and segmental motions of the macromolecule and relates to gas diffusion. This concept underlies the

dual sorption model that distinguishes permeant molecules sorbed in the free volume and those dissolved in the polymer matrix.²⁰ For oxygen in PET, the contribution of the Henry's law mechanism is negligible. Rather, sorption is the process of filling the holes of free volume, and the solubility should be proportional to the amount of free volume.

This interpretation of solubility permits a straightforward correlation between S and T_g . As a result of the long timescale required for glassy polymers to relax fully, gas transport typically occurs under nonequilibrium conditions wherein a polymer possesses more free volume than it would at equilibrium. Following the concepts of Vrentas and Duda,²¹ the volume of the nonequilibrium glassy polymer will be larger than the volume extrapolated from equilibrium by the excess-hole free volume (Fig. 4). The amount of excess-hole free volume can be estimated from the difference between the equilibrium and glassy specific thermal expansivities (e_e and e_g , respectively). Thus, the specific excess-hole free volume that is trapped within the glassy polymer at temperature T depends on the proximity to T_g as $\Delta v = (e_e - e_g)(T_g - T)$.^{22,23}

The correlation between T_g and oxygen solubility is demonstrated in Figure 5. According to Figure 4, consideration of oxygen sorption as the process of filling excess-hole free volume requires

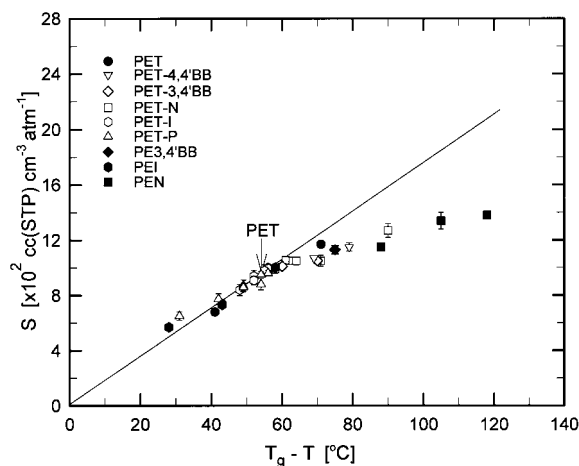


Figure 5. Relationship between solubility and the difference between the T_g and the test temperature: open symbols, measurements at 25 °C; solid symbols, measurements at other temperatures. Considering only copolymers of terephthalate with its isomers, the linear correlation extrapolated to $S = 0$ at $T = T_g$ with a slope of $17.2 \times 10^{-4} \text{ cc(STP) cm}^{-3} \text{ atm}^{-1} \text{ K}^{-1}$ ($R = 0.926$).

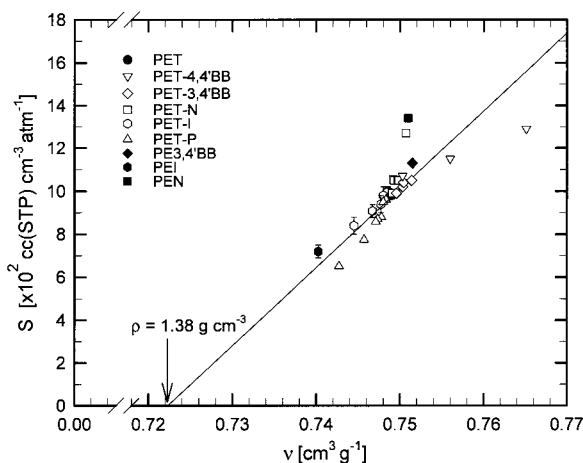


Figure 6. Relationship between solubility and specific volume ($\nu = \rho^{-1}$). Excluding copolymers with high concentrations of naphthalate or 4,4'-biphenylene, the linear correlation extrapolated to $S = 0$ at $\nu^{-1} = 1.38 \text{ g cm}^{-3}$, the density of the amorphous polymer with no free volume (ref. 1), with a slope of $3.6 \text{ cc(STP) g cm}^{-6} \text{ atm}^{-1}$ ($R = 0.846$).

extrapolation to $S = 0$ at $T = T_g$. The linear fit of the data points closest to T_g demonstrated this characteristic. The slope of $17.2 \times 10^{-4} \text{ cc(STP) cm}^{-3} \text{ atm}^{-1} \text{ K}^{-1}$ reflected the density d of oxygen sorbed in the free volume:

$$d = \frac{\nu\beta_1 P}{\Delta e} \left(\frac{M_w}{22,400} \right) \quad (2)$$

where ν is the specific volume of the polymer (taken as $0.749 \text{ cm}^3 \text{ g}^{-1}$), $\Delta e = e_e - e_g = 4.8 \times 10^{-4} \text{ cm}^3 \text{ g}^{-1} \text{ K}^{-1}$ for PET,²⁴ $P = 1 \text{ atm}$ is the ambient pressure of oxygen gas, and $M_w = 32$ for oxygen. The density of sorbed oxygen, $3.83 \times 10^{-3} \text{ g per cm}^3$ of free volume or about 2.7 atm, indicated that the sorbed oxygen was in the gaseous state.

The general observation that asymmetric polymers have higher density than the symmetric counterparts³ is another consequence of their lower T_g 's and, hence, lower free volume at ambient temperature. In conforming to this trend, the density of PET copolymers increased with the fraction of asymmetric comonomer (see Table II). The linear relationship between the specific volume of the amorphous polymer, $\nu = \rho^{-1}$, and oxygen solubility is illustrated in Figure 6. The solid line, with extrapolation to zero solubility giving the density of the amorphous polymer with zero accessible free volume, $\nu_0 = 1.38 \text{ g cm}^{-3}$, was

taken from a previous study of the oxygen permeability of PET.¹ The isomeric copolymers conformed to the linear relationship. Somewhat surprisingly, nonisomeric copolymers also fell on the line with significant deviation only for copolymers with high concentrations of naphthalate or 4,4'-BB.

The density of sorbed oxygen d was extracted from the slope of $3.6 \text{ cc(STP) g cm}^{-6} \text{ atm}^{-1}$ of the linear relationship in Figure 6 as

$$d = \nu\beta_2 P \left(\frac{M_w}{22,400} \right) \quad (3)$$

where the symbols have the same meaning as in eq 2. Eq 3 gives the density of sorbed oxygen as about $3.85 \times 10^{-3} \text{ g per cm}^3$ of free volume—the same as the value obtained from consideration of the T_g , eq 2. Thus, the gaseous state of sorbed oxygen is indicated. Carbon dioxide, another permeant gas that has been examined extensively, has a reported density in PET that is orders of magnitude higher, in-line with the condensed state.²⁵ This significant difference arises from the critical temperature, t_c . With t_c close to ambient temperature, the elevated pressure in the small holes of free volume is sufficient to cause condensation of carbon dioxide ($t_c = 31 \text{ }^\circ\text{C}$). This is not possible for oxygen ($t_c = -119 \text{ }^\circ\text{C}$) under ambient temperature test conditions.

Good correlation in Figure 6 indicates that oxygen sorption measured a common feature of the chemically similar aromatic polyesters used in the present study. Small deviations for some copolymers of naphthalate or 4,4'-BB were attributed to the effect of chemical structure on ν_0 , the specific volume of the amorphous polymer with zero solubility, rather than to fundamental differences in the characteristics of the accessible free volume. Hence, a unique interpretation of oxygen solubility was possible, wherein the difference between the specific volume of the amorphous polymer and the specific volume of the amorphous polymer with zero solubility was equal to the specific excess-hole free volume, ν_f . Moreover, ν_f was proportional to solubility S by the factor β_2 in the following equation:

$$\nu_f = \nu - \nu_0 = \frac{S}{\beta_2} \quad (4)$$

In this expression, it was not necessary for ν_0 to be the same for all the polyesters, only that the factor β_2 was the same.

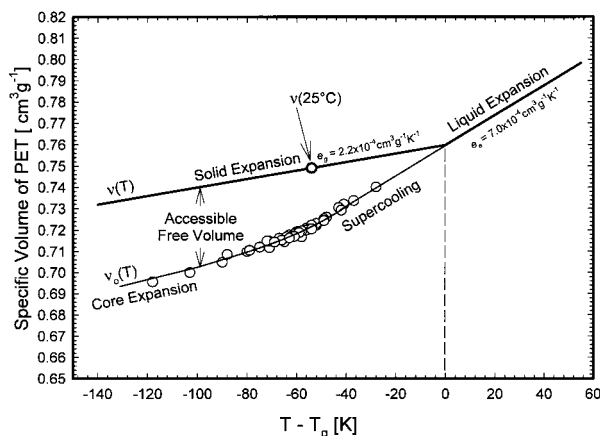


Figure 7. Specific volume–temperature relationship constructed for amorphous PET using oxygen solubility of various amorphous polyesters (Fig. 5) as a measure of accessible free volume.

It was then possible to create the volume–temperature behavior of an amorphous polyester. The example in Figure 7 is for PET. The specific volume line of the amorphous glass was constructed from the reference point defined by the amorphous density of 1.335 g cm^{-3} at $25 \text{ }^\circ\text{C}$ and T_g of $81 \text{ }^\circ\text{C}$ (Table II) and the specific thermal expansivity of $e_g = 2.2 \times 10^{-4} \text{ cm}^3 \text{ g}^{-1} \text{ K}^{-1}$. Reported experimental values and group-contribution calculations put the specific thermal expansivity of the amorphous glass at $e_g = 2.2 \times 10^{-4} \text{ cm}^3 \text{ g}^{-1} \text{ K}^{-1}$ for many aromatic polyesters including PEN.²⁴ The slope change at $T = T_g$ to the equilibrium liquid line was defined by the specific thermal expansivity of PET above its T_g , $e_e = 7.0 \times 10^{-4} \text{ cm}^3 \text{ g}^{-1} \text{ K}^{-1}$. For each data point in Figure 5, the specific excess-hole free volume ν_f was calculated from eq 4 and subtracted from the amorphous glass line of PET at the appropriate value of $T - T_g$. Calculated values of ν_f are included in Table II. The volume–temperature behavior of any other amorphous polyester could be obtained by shifting the reference point on the solid expansion line in Figure 7 according to the specific volume and T_g of the particular polymer.

The curve through the calculated points in Figure 7 extended the equilibrium liquid line below T_g . Consistent with the model in Figure 4, the excess-hole free volume became less dependent on temperature and indeed appeared to approach a constant value in the range of $0.04 \text{ cm}^3 \text{ g}^{-1}$ as the temperature decreased further below T_g . The approach to constant excess-hole free volume appeared experimentally as the decreasing slope of

the relationship between S and $T_g - T$ in Figure 5 for glassy polymers with higher T_g 's. Coincidence of the slope change with the postulated second-order transition at $T_g - 60 \text{ }^\circ\text{C}$ ^{26,27} raised speculation that solubility measurements revealed the equilibrium core expansion. In this interpretation, the supercooled glass core followed the equilibrium liquid-expansion line between T_g and $T_g - 60 \text{ }^\circ\text{C}$ and exhibited constant free volume below the transition in accordance with the classical Williams–Landel–Ferry interpretation.²⁸

Finally, diffusivity, which varies more than solubility from one polymer to another and therefore primarily determines differences in permeability, does not correlate with free volume from solubility despite the degree of chemical similarity among the polymers studied. This result suggests that the large scatter encountered in efforts to predict permeability of common gases in a wide array of glassy polymers by empirical application of the free-volume concept^{13,29} is inevitable and a consequence of factors other than free volume that affect diffusivity.

Diffusion Coefficient and Molecular Relaxation

Theories and models for the diffusion coefficient and its dependence on temperature generally have a basic premise that the diffusing molecule makes a successful diffusion jump of length δ with frequency ω . The diffusion coefficient characterizing a solid-state jump mechanism is³

$$D = \frac{\delta^2 \omega}{6} \quad (5)$$

The jump of the diffusing molecule from one equilibrium position to the next can be regarded as equivalent to passage of the system over a potential energy barrier expressed as an Arrhenius relationship with activation energy E_D

$$D = D_0 \exp\left(-\frac{E_D}{RT}\right) \quad (6)$$

The dynamic free volume that controls jump motion of permeant molecules between static free-volume cavities derives from accessible conformational changes and segmental motions of the polymer chain. In a glassy polymer, it seems reasonable that these thermal rearrangements would manifest themselves as sub- T_g relaxation

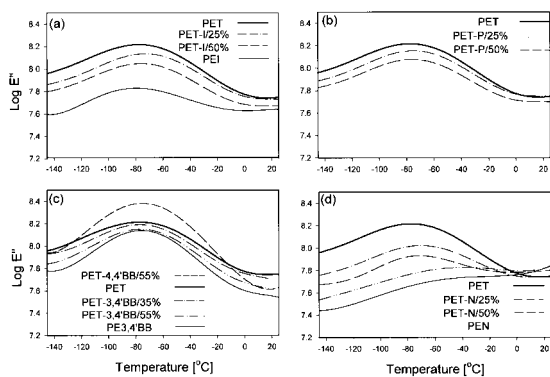


Figure 8. Effect of copolymerization on $\log E''$ in the γ -relaxation region: (a) PET-I copolymers, (b) PET-P copolymers, (c) PET-BB copolymers, and (d) PET-N copolymers.

processes. Indeed, there exists at least one report of a relationship between oxygen diffusivity and the prominent subambient relaxation observed in aromatic polyesters.⁹

Relaxation behavior of the copolyesters is reported as $\log E''$, which is a more fundamental viscoelastic quantity than $\tan \delta$ (Fig. 8). The PET homopolymer exhibited a pronounced γ -relaxation peak at about -75 °C (1 Hz). It is generally thought that the broad peak encompasses several relaxation processes involving both methylene groups and ester linkages.^{30–32} Most of the polymers in the present study exhibited a γ relaxation at approximately the same temperature as PET. Changes in chemical structure affected primarily the relaxation intensity. As reported previously, the asymmetric isomers (isophthalate and phthalate) lowered the relaxation strength.³³ Asymmetric 3,4'BB also lowered the relaxation strength, although not as much as isophthalate and phthalate. However, copolymerization with symmetric 4,4'BB increased the intensity. Relaxation curves of the copolymers in the γ -relaxation region were intermediate between those of the corresponding homopolymers. Replacing the single phenyl group with a naphthalate group increased the temperature of the γ relaxation in PEN to -50 °C (1.0 Hz). Relaxation mechanisms similar to those of PET, that is, local motion of methylene groups and ester linkages, were proposed with the shift in temperature attributed to increased local chain rigidity.^{34,35}

In testing for a relationship between relaxation strength and diffusivity, the relaxation intensity $I_{E''}$ was taken as the area under the $\log E''$ curve evaluated between -145 °C and ambient temper-

ature. The diffusivity showed an excellent logarithmic dependence on the relative relaxation intensity defined as $[1 - (I_{E''}/I_{E'',PET})]$ where $I_{E''}$ is the relaxation intensity of the copolymer, and $I_{E'',PET}$ is the relaxation intensity of PET (Fig. 9). The result verifies the previous finding of a correspondence between oxygen diffusivity and γ -relaxation strength⁹ and poses the correlation as a general feature of aromatic copolyesters related to PET. The generality beyond aromatic copolyesters remains to be tested.

If indeed the dynamic free volume arises from the same thermally activated chain motions as the γ relaxation, the activation energy for diffusion (E_D) should be comparable to the activation energy of the γ relaxation (E_γ). Additional tests were performed to obtain the temperature dependence of P and D . The temperature dependence of P for oxygen in PET is available in the literature.⁹ The experimental data from the present study smoothly extends previous results to higher temperatures resulting in an activation energy for permeability (E_P) of 30 kJ mol⁻¹ (Fig. 10).

Although the present study utilized a rather narrow temperature interval, 10 – 40 °C, the correlation in P suggested that it was sufficient for determining the activation energy. Activation energies for oxygen diffusion in PET, PEI, and PEN were 40 , 43 , and 44 kJ mol⁻¹, respectively (Fig. 11). The activation energy of the γ relaxation is available in the literature for several of the homopolymers (see Table III). Good correlation in activation energies gave credence to the idea that dynamic free volume for oxygen diffusion and the dynamic mechanical γ relaxation originate from

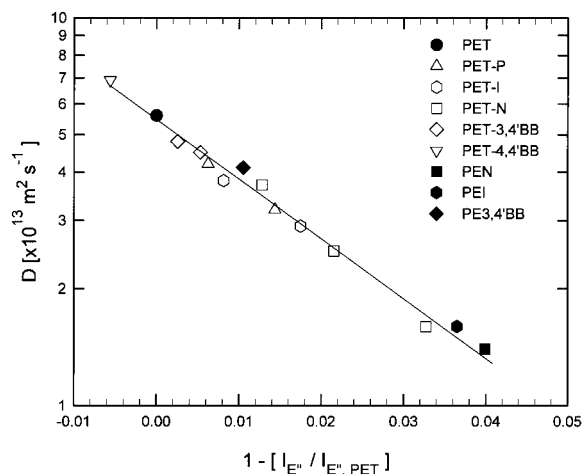


Figure 9. Relationship between diffusivity and the relative intensity of the γ relaxation.

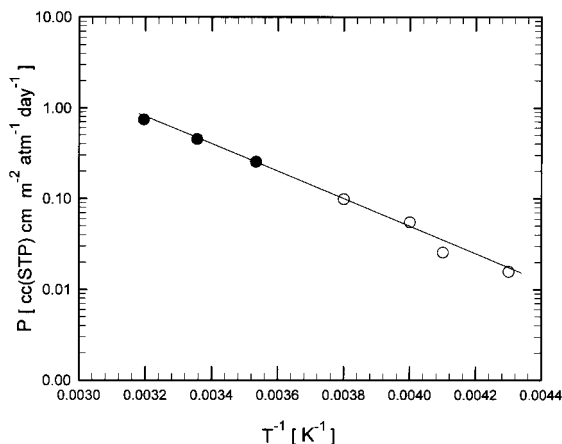


Figure 10. Temperature dependence of permeability for PET: solid symbols from this study; open symbols from ref. 9. From the linear relationship, $E_P = 30 \text{ kJ mol}^{-1}$ ($R = 0.998$).

the same thermally activated molecular motions. Data taken from the literature for polycarbonate and included in Table III suggest that the relationship between D and sub- T_g relaxations may be a common feature of oxygen diffusion in glassy aromatic polymers.^{36,37}

The complexity of the γ relaxation has sometimes led investigators to identify specific components with *trans* and *gauche* conformers of the glycol,^{17,30,31} with somewhat different activation energies.³⁸ Thus, E_γ for *trans* conformers is higher than E_D , but E_γ for *gauche* conformers are lower. The differences between and in Table III may indicate that a single value for the activation energy does not adequately describe the molecular motions. Diffusion and mechanical relaxation

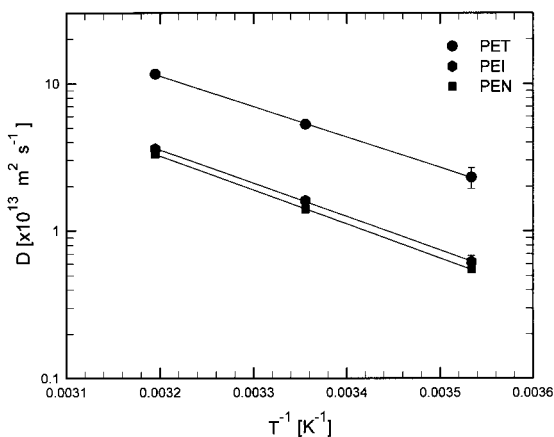


Figure 11. Temperature dependence of diffusivity for PET, PEI, and PEN.

Table III. Activation Energies for Oxygen Permeability and Diffusivity

Material	E_P (kJ mol ⁻¹)	E_D (kJ mol ⁻¹)	E_γ (kJ mol ⁻¹)
PET	30 32.5 ^a	40	49.8 ^b 52.1 ^c <i>trans</i> 32.8 ^c <i>gauche</i>
PEI	34	43	56.9 ^d
PEN	30	44	58.2 ^d
PC		40	54.3 ^e

^a Ref. 36.

^b Ref. 35.

^c Ref. 38.

^d Ref. 37.

^e Ref. 34.

may emphasize somewhat different parts in a distribution of molecular motions with a spectrum of activation energies. Some γ -relaxation motions may be more effective than others for enabling jump motion of permeant molecules between static free-volume cavities. An increase in *trans* conformers has been linked to lower oxygen permeability,^{39,40} which may explain why E_D correlates better with the activation energy for *gauche* conformers.

CONCLUSION

Systematic changes in the chemical structure of PET by copolymerization made it possible to test free-volume concepts in which permeation of a small gas molecule through a glassy polymer is viewed as proceeding by occasional jumps (dynamic free volume) between neighboring cavities (static free volume). The correlation between solubility S and T_g confirms the dependence of S on the total volume of cavities in the polymer matrix (static free volume) and the essential independence of thermally accessible motions of the polymer chain. The correlation between diffusivity D and the subambient γ relaxation demonstrates that the conformational changes and segmental motions of the macromolecule (dynamic free volume) from which D derives are manifest as sub- T_g relaxation processes. This characteristic may be general for aromatic polyesters.

The authors thank Prof. S. Nazarenko for the many stimulating discussions. This research was generously supported by the KOSA Corp. and the National Science

Foundation, Grants DMR 9975774 and DMR 9986467. Support from Modern Controls, Inc. for development of a facility for gas-transport studies at Case Western Reserve University is gratefully acknowledged.

REFERENCES AND NOTES

1. Sekelik, D. J.; Stepanov, S. V.; Nazarenko, S.; Schiraldi, D.; Hiltner, A.; Baer, E. *J Polym Sci Part B: Polym Phys* 1999, 37, 847.
2. Qureshi, N.; Stepanov, S. V.; Schiraldi, D.; Hiltner, A.; Baer, E. *J Polym Sci Part B: Polym Phys* 2000, 38, 1679.
3. Pixton, M. R.; Paul, D. R. In *Polymeric Gas Separation Membranes*; Paul, D. R.; Yampol'skii, Yu. P., Eds.; CRC: Boca Raton, FL, 1994; Chapter 3, pp 83–153.
4. Aitken, C. L.; Koros, W. J.; Paul, D. R. *Macromolecules* 1992, 25, 3424.
5. Sykes, G. F.; St. Clair, A. K. *J Appl Polym Sci* 1986, 32, 3725.
6. Stern, S. A.; Mi, Y.; Yamamoto, H. *J Polym Sci Part B: Polym Phys* 1989, 27, 1887.
7. Tanaka, K.; Kita, H.; Okamoto, K.; Nakamura, A.; Kusuki, Y. *Polym J* 1990, 22, 381.
8. Coleman, M. R.; Koros, W. J. *J Membr Sci* 1990, 50, 285.
9. Light, R. R.; Seymour, R. W. *Polym Eng Sci* 1982, 22, 857.
10. Sheu, F. R.; Chern, R. T. *J Polym Sci Part B: Polym Phys* 1989, 27, 1121.
11. Zhang, T.; Litt, M. H.; Rogers, C. E. *J Polym Sci Part A: Polym Chem* 1994, 32, 1351.
12. Boyer, R. F. *Rubber Rev* 1963, 36, 1304.
13. Thran, A.; Kroll, G.; Faupel, F. *J Polym Sci Part B: Polym Phys* 1999, 37, 3344.
14. Hill, A. J.; Weinhold, S.; Stack, G. M.; Tant, M. R. *Eur Polym J* 1996, 32, 843.
15. Kotliar, A. M. *J Polym Sci Part D: Macromol Rev* 1981, 16, 367.
16. Asrar, J. *J Polym Sci Part A: Polym Chem* 1999, 37, 3139.
17. Uralil, F.; Sederel, W.; Anderson, J. M.; Hiltner, A. *Polymer* 1979, 20, 51.
18. Theodorou, D. N. In *Diffusion in Polymers*; Neogi, P., Ed.; Marcel Dekker: New York, 1996; Chapter 2, pp 67–142.
19. Stern, S. A. *J Membr Sci* 1994, 94, 1.
20. Stern, S. A.; Trohalaki, S. In *Barrier Polymers and Structures*; ACS Symposium Series 423; Koros, W. J., Ed.; American Chemical Society: Washington, DC, 1990; Chapter 2, pp 22–59.
21. Vrentas, J. S.; Duda, J. L. *J Appl Polym Sci* 1978, 22, 2325.
22. Duda, J. L.; Zielinski, J. M. In *Diffusion in Polymers*; Neogi, P., Ed.; Marcel Dekker: New York, 1996; Chapter 3, pp 143–171.
23. Platé, N.; Yampol'skii, Y. In *Polymeric Gas Separation Membranes*; Paul, D. R.; Yampol'skii, Yu. P., Eds.; CRC: Boca Raton, FL, 1994; Chapter 4, pp 155–207.
24. Van Krevelen, D. W. *Properties of Polymers*, 3rd ed.; Elsevier: Amsterdam, 1997; Chapter 4, pp 71–107.
25. Koros, W. J.; Paul, D. R. *J Polym Sci Polym Phys Ed* 1978, 16, 1947.
26. Gibbs, J. H.; DiMarzio, E. A. *J Chem Phys* 1958, 28, 373.
27. Miller, A. A. *J Polym Sci Part A: Gen Pap* 1963, 1, 1857.
28. Ferry, J. D. *Viscoelastic Properties of Polymers*, 3rd ed.; Wiley: New York, 1980; Chapter 11, pp 264–320.
29. Park, J. Y.; Paul, D. R. *J Membr Sci* 1997, 125, 23.
30. Illers, K. H.; Breuer, H. *Journal Colloid Science* 1963, 18, 1.
31. Armeniades, C. D.; Baer, E. *J Polym Sci Part A-2: Polym Phys* 1971, 9, 1345.
32. Coburn, J. C.; Boyd, R. H. *Macromolecules* 1986, 19, 2238.
33. Yip, H. K.; Williams, H. L. *J Appl Polym Sci* 1976, 20, 1217.
34. Chen, D.; Zachmann, H. G. *Polymer* 1991, 39, 1612.
35. Ezquerro, T. A.; Baltà-Calleja, R. J.; Zachmann, H. G. *Acta Polym* 1993, 44, 18.
36. Muruganandam, N.; Koros, W. J.; Paul, D. R. *J Polym Sci Part B: Polym Phys* 1987, 25, 1999.
37. Walton, J. H.; Lizak, M. J.; Conradi, M. S.; Gullion, T.; Schaefer, J. *Macromolecules* 1990, 23, 416.
38. Berticat, P.; Chatain, D.; Monpagens, J. C.; Lacabanne, C. *J Macromol Sci Phys* 1978, B15, 549.
39. Slee, J. A.; Orchard, G. A. J.; Bower, D. I.; Ward, I. M. *J Polym Sci Part B: Polym Phys* 1989, 27, 71.
40. Orchard, G. A. J.; Spiby, P.; Ward, I. M. *J Polym Sci Part B: Polym Phys* 1990, 28, 603.